ADVANCED FUNCTIONAL MATERIALS
www.afm-journal.de

Soft Processing of Graphene Nanosheets by Glycine-Bisulfate Ionic-Complex-Assisted Electrochemical Exfoliation of Graphite for Reduction Catalysis

*Kodepelly Sanjeeva Rao, Jaganathan Sentilnathan, Hsun-Wei Cho, Jih-Jen Wu, and Masahiro Yoshimura**

This study demonstrates a mild, environmentally friendly, and cost-effective soft processing approach for the continuous synthesis of high-quality, few-layer graphene nanosheets. This has been achieved via electrochemical exfoliation of graphite, using an environmentally friendly glycine-bisulfate ionic complex and was performed under ambient reaction conditions. Graphene nanosheets with 2–5 layers were obtained under optimized exfoliation conditions using a 15 wt% glycine-bisulfate (aqueous) solution, with working biases of +1 V and +3 V applied for 5 min. The role of the glycine-bisulfate ionic complex in the electrochemical exfoliation process was confirmed through comparison with a control experiment using only sulfuric acid as the electrolyte. A plausible electrochemical exfoliation mechanism that involves the formation of surface molecule nuclei via the polymerization of intercalated monomeric HSO_4^- and SO_4^{2-} ions is proposed. The ionic complex plays a key role in the anodic graphite exfoliation via electrochemical-potential-induced intercalation, leading to an efficient expansion of graphite sheets via the insertion of oxygen functional groups.

1. Introduction

The outstanding mechanical, electrical, optical, and thermal properties[1–4] of graphene, along with its many potential applications, has led to an exponential growth in graphene-based materials research over the past few years. Numerous functional graphene materials have now been synthesized using different structural motifs including metal-organic frameworks, polymers, biomaterials, organic crystals, and inorganic nanostructures. Several synthetic approaches, such as chemical vapor deposition (CVD),[5–7] micromechanical exfoliation,[5,8] epitaxial growth on SiC,[8,9] solution route wet chemical exfoliation,[10] sonochemical liquid-phase exfoliation,[8,11] and volatile-agent-assisted intercalation-expansion,[9,12] have been applied in the preparation of these graphene-based materials.

Solution processing[8,9,12–22] is a particularly attractive approach due to its low cost and environmental friendliness. The electrochemical exfoliation of graphite[23–34] is one such example of solution based processing that has been used for the direct preparation of low-defect graphene nanosheets (GNSs). Within this broader processing regime the use of ionic liquids[23–25] are of particular interest due to their suitability as electrolytes. Previously, Liu et al.[23] and Lu et al.[24] have demonstrated the preparation of graphene via the electrochemical intercalation of PF_6^- and BF_4^- anions into graphite layers using alkylimidazolium hexafluorophosphate ($RIMPF_6$) and alkylimidazolium tetrafluoroborate ($RIMBF_4$) ionic liquids. Ionic liquids have several merits, including negligible vapor pressure, low toxicity, high chemical and thermal stability, and ease of availability.[23–25] Whilst ionic-liquid-assisted electrochemical methods have several advantages, they also suffer from a number of drawbacks. Ionic liquids require non-soft (uncommon in natural/biological systems, expensive/complexity in handling) starting materials along with complex/additional procedures, higher voltages, higher costs, and suffer some disruption to the electronic properties of produced graphene as a result of ionic liquid functionalization.[23] Alternatively, graphite exfoliation in acidic electrolytes provides good quality graphene, but a large number of oxygen functional groups are inserted via the acid-assisted heavy oxidation of graphite.[32] Our recently dveloped[31] peroxide ions assisted exfoliation method has several advantages, although it does require the use of strong alkaline solutions. Therefore, the development of simple, low-cost, environmental friendly, yet highly efficient methods for the preparation of good quality graphene is still required for practical applications. We have found that glycine-bisulfate ($Gly \cdot HSO_4$) is such a candidate, particularly as glycine is a natural biocompatible material.

The formation of $Gly \cdot HSO_4$ ionic complex in aqueous solutions is a 100% atom-economical process (the molecular mass

Dr. K. S. Rao, Dr. J. S. Nathan, Prof. M. Yoshimura
Promotion Center for Global Materials Research (PCGMR)
Department of Material Science and Engineering
National Cheng Kung University, 70101, Taiwan
E-mail: yoshimur@mail.ncku.edu.tw
Mr. H-W. Cho, Prof. J-J. Wu
Department of Chemical Engineering
National Cheng Kung University, 70101, Taiwan

DOI: 10.1002/adfm.201402621

of Gly·HSO_4 is equal to the total molecular mass of starting glycine and H_2SO_4), being low-cost, and environmentally friendly, and has been applied previously for organocatalysis.[35–37] To date, it has not been applied in the electrochemical processing of graphene. The study presented here utilizes Gly·HSO_4 ionic complex as a mild, cost-effective chemical agent for the efficient electrochemical exfoliation of graphite for the first time. We present a comprehensive characterization of the exfoliated GNSs including a plausible and detailed proposal explaining the exfoliation mechanism. This work illustrates an efficient soft processing[38] method for the preparation of high quality GNSs.

2. Results and Discussion

2.1. Optimization of Exfoliation Conditions

The process developed for the preparation of GNSs is presented in **Figure 1**. To prepare the Gly·HSO_4 ionic complex used for exfoliation experiments, an equimolar mixture of glycine and H_2SO_4 in aqueous solution was stirred for 1 h at room temperature (Figure 1a).[35,39] A schematic diagram of the electrochemical setup is presented in Figure 1b. Within the reaction vessel a graphite anode was placed parallel to a platinum cathode and exfoliation experiments were performed under ambient reaction conditions. Initial experiments were conducted to compare the use of H_2SO_4 alone as the electrolyte with that of the Gly·HSO_4 ionic complex, these were done using a Gly·HSO_4 to water (by weight) ratio of 4:96 under different bias voltages. Experiments were then performed across a further range of Gly·HSO_4 to water weight ratios (4:96, 9:91, 15:85, and 40:60). The corresponding products are denoted as GNS4, GNS9, GNS15, and GNS40, with obtained yields of 0.8, 1.3, 2.2, and 2.4 g L^{-1}, respectively (see Table S1, Supporting Information for full details).

The optimal exfoliation conditions for the preparation of high-quality, few-layer GNSs were found to be a Gly·HSO_4 to water ratio of 15:85 and working biases of +1 V and +3 V applied for 5 min (GNS15, Table S1, ESI). Photographs of the exfoliated GNS15 directly in electrolyte solution and also re-dispersed in N-methyl-1-pyrrolidone (NMP) after purification are shown in Figure 1c. No exfoliation was observed in a control experiment conducted with a graphite cathode under the optimal anodic exfoliation conditions. Another control experiment, which utilized only H_2SO_4 as the electrolyte, did not produce GNSs, but instead formed a graphene oxide (GO)-like material (Table S1, Supporting Information). The Gly·HSO_4 ionic complex is mild yet superior to the mixed electrolyte H_2SO_4 + KOH (pH 1.2) for the exfoliation of graphite[32] and better than aqueous NaOH + H_2O_2 reported in our previous work.[31]

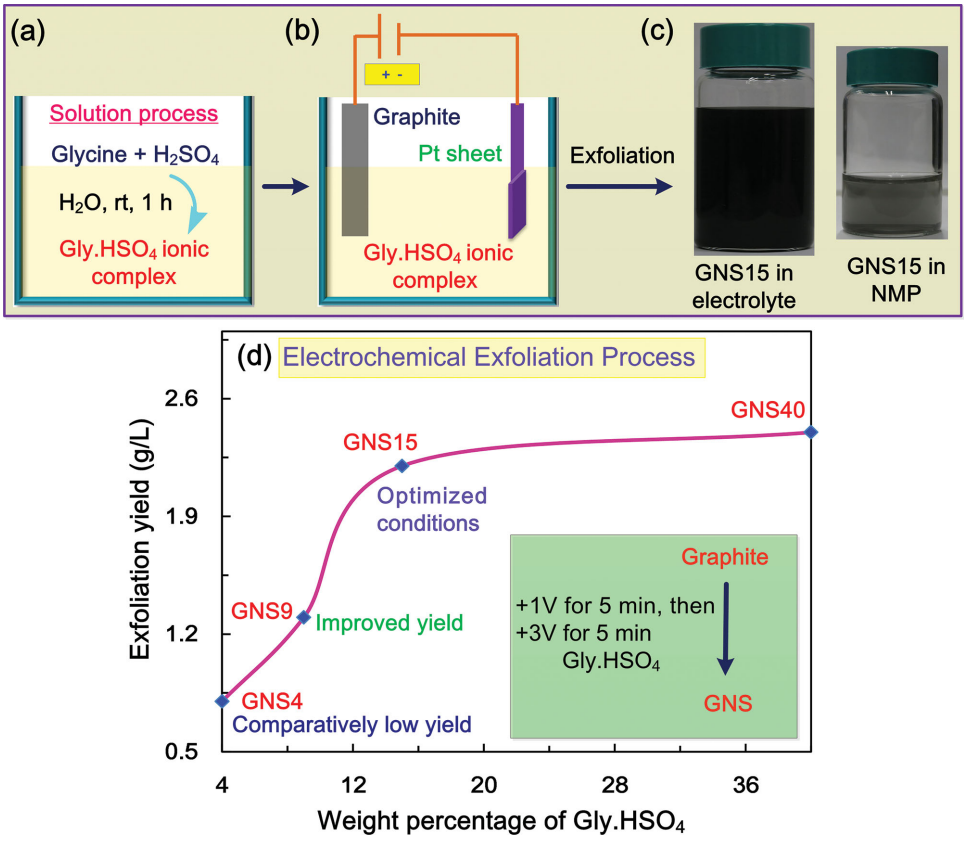

Figure 1. Preparation process of GNSs. a) A simple solution-process approach for Gly·HSO_4 ionic complex preparation in aqueous solution.[35] b) Diagram of electrochemical experimental setup. c) Photographs of GNS15 directly in electrolyte (left) and re-dispersed in NMP after purification (right). d) Exfoliation yields versus weight ratios of Gly·HSO_4 ionic complex to water used in exfoliation experiments.

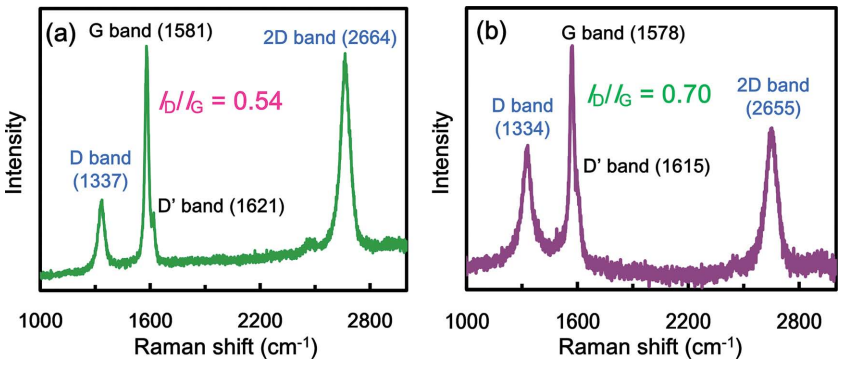

Figure 2. Raman spectra of a) graphite and b) GNS15 recorded at a laser excitation wavelength of 633 nm.

2.2. Properties of GNS15

The Raman spectrum of GNS15 was compared with that of pure graphite (**Figure 2**). The D band (related to disordered SP^3 structures) and the doubly degenerate (TO and LO) phonon E_{2g} mode G band (related to vibration of in-plane SP^2 π-network structure in a two-dimensional hexagonal lattice) of graphite normally appear at 1337 cm^{-1} and 1581 cm^{-1}, respectively. Whereas the D and G bands of GNS15 appear at 1334 cm^{-1} and 1578 cm^{-1}, respectively. The increased D band intensity of GNS15 indicates the formation of defects[14,26] such as adatoms, vacancies, and grain boundaries, formed most likely during electrochemical exfoliation process. The D′ shoulder bands (corresponding to disorder of edge carbons) appears at 1621 cm^{-1} and 1615 cm^{-1} for graphite and GNS15, respectively. The increased D′ band intensity of GNS15 indicates an increase in disorder of the edge carbons via the formation of ripples, dislocations or charged impurities.[26] The 2D bands (related to disorder-induced defects) of graphite and GNS15 appear at 2664 cm^{-1} and 2655 cm^{-1}, respectively. The defects formed in the GNS15 during exfoliation process increase the D band intensity and reduce the 2D and G bands intensities.[14] The 2D/G ratio of GNS15 (1.1) is good agreement with the graphene (1.2) prepared via submerged liquid plasma process by our group.[14] The D band to G band ratio (I_D/I_G)[40,41] of graphite and GNS15 are 0.54 and 0.70, respectively. The higher I_D/I_G value of GNS15 is likely due to structural defects formed during the exfoliation process. Comparison of the Raman spectra of graphite and GNS15 suggest the formation of high-quality graphene under the optimal mild exfoliation conditions. The Raman results of GNS15 are also in good agreement with high-quality graphene reported by Lu et al.[24]

Transmission electron microscopy (TEM) results of GNS15 are summarized in **Figure 3**. Figure 3a shows a low-magnification TEM image of GNS15 drop-casted onto a lacey carbon grid. The high-resolution TEM (HR-TEM) image of GNS15 shows the intermixing of defect-free and disordered domains (Figure 3b). These defect-free and disordered domains are shown at higher magnification in Figure 3c. Regarding the quality of GNS15, π-bonded carbon frameworks with few defects can be seen in the carbon lattice patterns (Figure 3d). The HR-TEM analysis also indicates the presence of few-layer graphene with 2–5 layers (Figures 3e-f). The statistical distribution of graphene sheet layers was obtained by

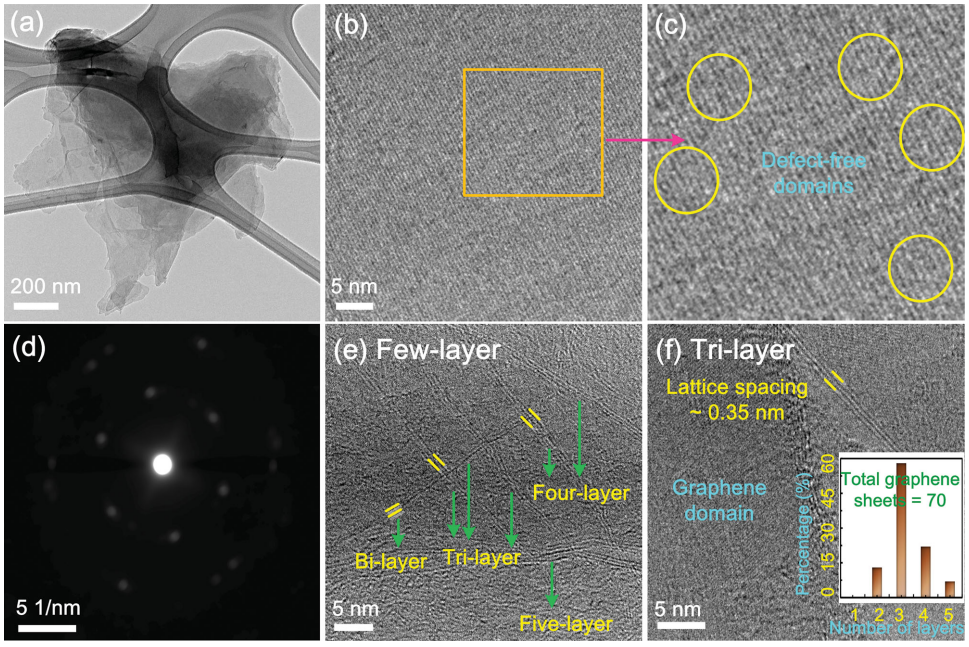

Figure 3. TEM analysis of GNS15 structure. a) Low-magnification TEM image of GNS15 drop-casted on lacey carbon grid. b) HR-TEM image of GNS15. c) High magnification of b) showing defect-free domains. d) Selected-area electron diffraction (SAED) pattern of carbon lattice. e, f) HR-TEM images of few-layer graphene and statistical distribution of graphene sheet layers (Inset of figure 3f).

evaluating a large number of HR-TEM images obtained from almost 70 graphene sheets. The distribution data shows that GNS15 consists of approximately 13% bi-layer, 48% tri-layer, 32% four-layer and 7% fiver-layer graphene nanosheets (Inset of Figure 3f). The carbon lattice spacing is around 0.35 nm, which is close to that reported in the literature.[24] This indicates the presence of few oxygen functional groups in GNS15. The appearance of an intense 2D band at 2660 cm^{-1} in the Raman spectrum of GNS15 also indicates the presence of few-layer graphene, further supported in literature,[42] leading us to believe the nanoscale morphology and the atomic structure of the carbon frameworks of GNS15 are of high quality.

X-ray photoelectron spectroscopy (XPS) studies also suggest the high quality of GNS15, the level and kind of functional groups inserted (**Figure 4**). The presence of carbon and oxygen in graphite and GNS15 is confirmed by a wide-scan XPS spectrum (Figure 4a). The starting graphite material contains carbon and oxygen in a ratio of 98.5:1.5, whereas exfoliated GNS15 contains carbon and oxygen in a ratio of 89:11, indicating the insertion of some oxygen functional groups during the exfoliation process.

The C1s spectrum of graphite and GNS15 shows an intense band at 284.8 eV corresponding to C-C bonds (Figure 4b-c). Appearance of a band at 285.9 eV in C1s spectrum of graphite indicating the presence of C-O functional groups (Figure 4b). For the GNS15, an increased intensity of the band at 286.3 eV corresponds to C-O bonds (related to hydroxyl/phenolic/epoxide groups) and the appearance of a new band (in comparison to the starting graphite) at 288.8 eV corresponds to C = O bonds (related to carboxylic acid groups) indicating the insertion of oxygen functional groups during the exfoliation process. These results are in good agreement with the literature reports[31,43–45] and suggest that GNS15 is graphene in nature as it appears to consist of graphene sheets with low level (11%) of oxygen groups unlike graphene oxide or even graphene.[22]

The Fourier transform infrared (FT-IR) spectrum of the starting graphite indicates the presence of very few oxygen functional groups, with peaks at 1000 cm^{-1} and 3340 cm^{-1} corresponding to C-O/CO-H (stretching) and CO-H (bending), respectively (Figure 4d, I). The peak corresponding to the π-carbon framework is at approximately 1580 cm^{-1} (C = C stretching). The FT-IR spectrum of GNS15 shows corresponding peaks at 1580 cm^{-1} (C = C, C = O stretching) and 3340 cm^{-1} (CO-H bending) (Figure 4d, II). The relatively high intensity of the peak at around 1000 cm^{-1} (C-O/CO-H stretching) indicates the presence of the hydroxyl/phenolic/alkoxy functional groups, which are in good agreement with the research work of others.[46] These results confirm the insertion of oxygen functional groups, such as hydroxyl/phenolic, alkoxy, and carboxyl groups, during the exfoliation process. These FT-IR results confirm our findings from our XPS results. Therefore, based on our XPS and FT-IR results, we propose the structural features of GNS15 contain epoxide, hydroxyl, phenolic, and carboxylic functional groups, as illustrated in Figure S3, ESI.

2.3. Proposing Exfoliation Mechanism

Various research groups have proposed anodic graphite electrochemical exfoliation mechanisms using a range of

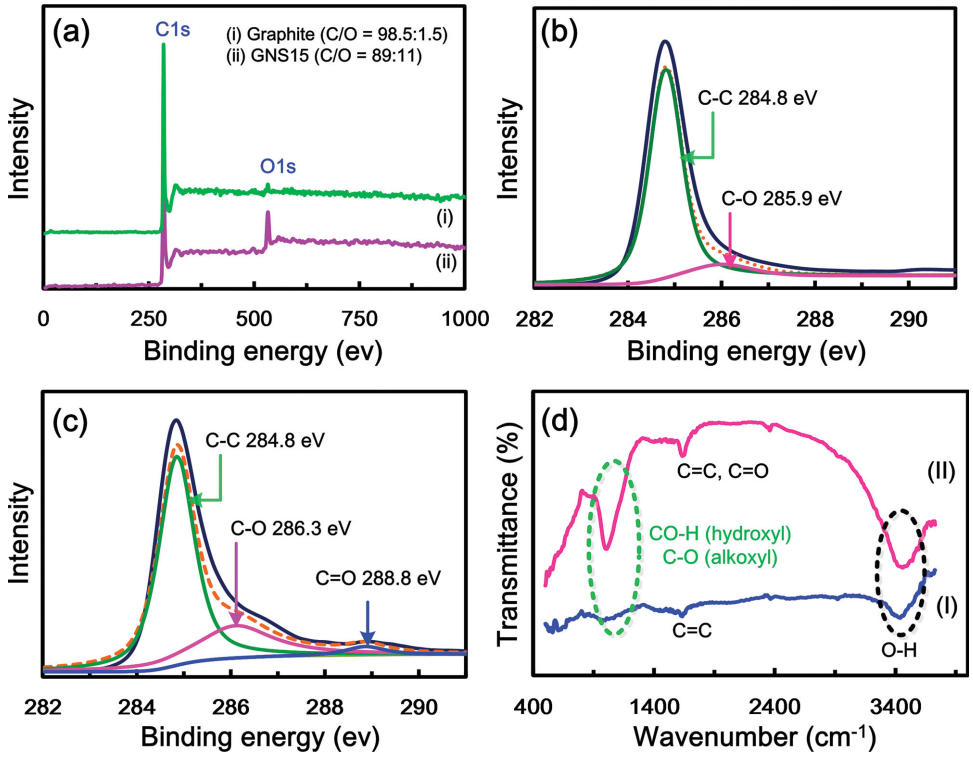

Figure 4. XPS analysis results. a) XPS spectra of i) graphite and ii) GNS15 in wide-range scan. C1s core-level spectra of b) graphite and c) exfoliated GNS15, showing insertion of some oxygen functional groups. d) FT-IR spectra of I) graphite and II) GNS15, showing good agreement with XPS results.

processing parameters.[25,27–34] Most electrochemical mechanisms assume that simple anions generated from electrolytes can directly undergo intercalation when a potential is applied across two electrodes,[28] i.e.,HSO_4^- and SO_4^{2-} anions generated from H_2SO_4 electrolyte undergo intercalation at the graphite anode.[28] The intercalation of these anions may also promote depolarization and the subsequent expansion of the graphite anode,[48,49] leading to further exfoliation. Exfoliation can also be induced by electrochemical potentials (electric field force),[25] therefore the controlled synthesis of graphene can also be achieved by varying the potential.[47] Recently, Parvez et al.[50] studied the electrochemical exfoliation of graphite and proposed a plausible exfoliation mechanism. They suggested that the reduction of intercalated SO_4^{2-} ions produces SO_2 gas, and the evolution of gas bubbles creates large forces among graphite layers, leading to exfoliation. However, it is not clear how enough monomeric SO_2 molecules are able to accumulate to create large enough bubbles and in turn large forces among the graphite layers to cause exfoliation. The formation of an SO_2 gas bubble requires a huge number of SO_4^{2-} ions (e.g., a 100-nm SO_2 bubble comprises 10^3 monomeric SO_2 molecules).

The present study proposes an electrochemical exfoliation mechanism based on the experimental results and published literature.[25,27–35,47–49] The mechanism is shown in **Figure 5**.

a) The aqueous solution of glycine reacts with equimolar H_2SO_4 to form the Gly·HSO_4 ionic complex.[35]

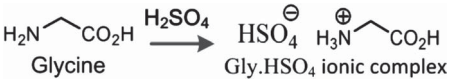

b) The Gly·HSO_4 ionic complex facilitates the intercalation of HSO_4^- and SO_4^{2-} ions into graphite (anode) sheets. The electrochemical potential also helps the intercalation of these ions, leading to exfoliation.[31]

c) The intercalated monomeric HSO_4^- and SO_4^{2-} ions undergo polymerization, forming dimers, trimmers, and their clusters via repeated addition of monomeric ions.

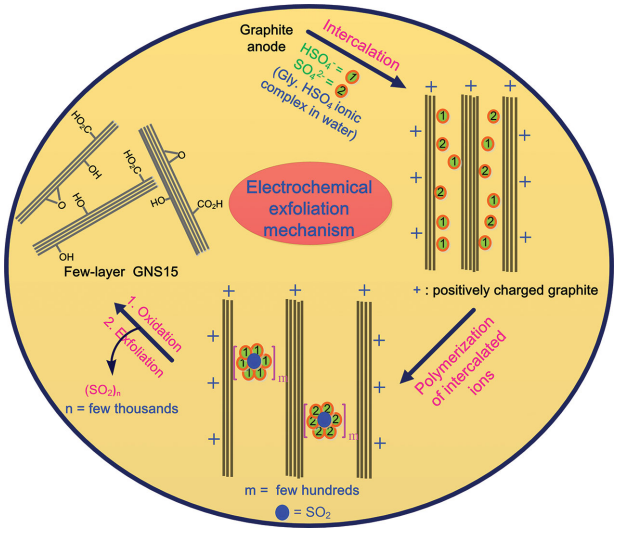

Figure 5. Schematic of proposed electrochemical exfoliation mechanism.

d) When such ion clusters exceed a certain size, the internal species enveloped by surface ions becomes isolated, and they become reduced to neutral molecules.

e) Surface molecule nuclei form via the addition of many monomeric ions, eventually forming large $(SO_2)_n$ gas bubbles, where n is in thousands.

f) The oxidation of graphite by such ionic species leads to the formation of oxygen functional groups on the graphite surfaces, which in turn lead to the evolution of large $(SO_2)_n$ gas bubbles.

g) The large forces among graphite layers created by large $(SO_2)_n$ gas bubbles facilitate the efficient exfoliation of graphite sheets into GNSs.

h) Additionally, hydroxyl (·OH) and oxygen (·O) radicals generated from the anodic oxidation[14] of water are involved in the opening of graphite edge sheets via the oxidation of edge sites and facilitate the intercalation of HSO_4^- and HSO_4^{2-} ions. Subsequently, depolarization and expansion of the graphite anode occur.[31]

This exfoliation mechanism includes several hypotheses. Experimental results reveals that aqueous Gly·HSO_4 ionic complex is an efficient exfoliating agent. The conversion process of SO_2 gas into Na_2SO_3 by passing through aqueous NaOH solutions is one of the best methods to avoid the environmental pollution. Moreover H_2SO_4 itself is one of a very common chemicals, then it can be rather easily precipitated as $CaSO_4$ by $Ca(OH)_2$ or even $CaCO_3$, which are cheaper and safer chemicals. The present method is more efficient than our recently reported[31] exfoliation method that uses aqueous NaOH + H_2O_2 because it is faster, low-cost, environmental friendly and a simple production process. We believe our exfoliation method is one of the most efficient methods available when considering our systematic analysis and comparison with other reported methods shown in Table S2, Supporting Information.

2.4. Reduction Catalysis

The reduction of carbonyl compounds such as esters to their corresponding alcohols is a common reaction in organic chemistry[51] and important to the pharmaceutical industry. Traditional reduction methods[51] such as catalytic hydrogenation and chemical reduction often involve complex operational procedures, long reaction times, toxic solvents/reagents, and sensitive to processing conditions. Here, we demonstrate the reduction of a carbonyl compound (easily detectable ethyl benzoate) using aqueous $NaBH_4$ catalyzed by gold nanocrystals (AuNCs) and a GNS-AuNCs hybrid (**Figure 6**). Aqueous $NaBH_4$ has been applied in our previous work for benzaldehyde[52] reduction catalyzed by a nitrogen-functionalized graphene-AuNCs hybrid.

The reaction evolution was monitored using time-dependent ultraviolet-visible (UV–Vis) spectroscopy. It was found that only AuNCs were catalytically inactive (Figures 6a–b), whilst enhanced catalytic efficiency of the GNS-AuNCs hybrid was observed (Figure 6c). The GNS-AuNCs hybrid catalysis required only 100 seconds for completion, whereas AuNCs required

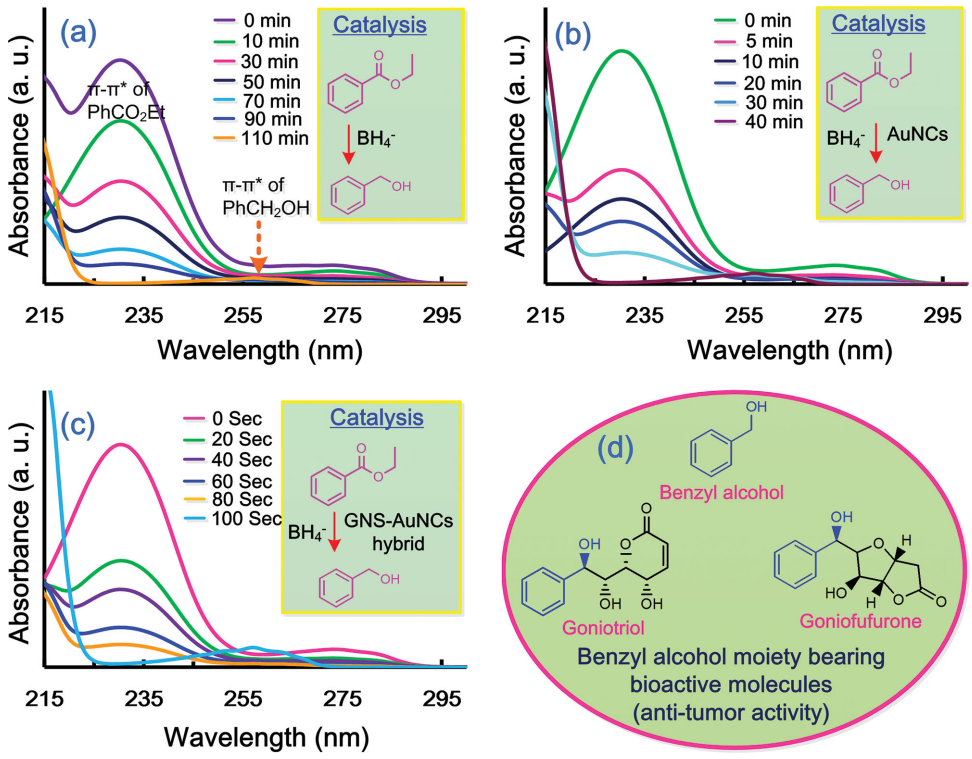

Figure 6. Investigation of ethyl benzoate reduction catalysis by time-dependent UV–Vis spectra for a) blank, b) AuNCs, and c) GNS-AuNCs hybrid in aqueous media at 25 °C. d) Structures of bioactive molecules that contain benzyl alcohol core moiety.

40 min. Initially the ethyl benzoate UV–Vis spectra showed peaks at 230 (C = C) and 275 nm (C = O). After the reaction was complete, these peaks disappeared and a new peak appeared at 259 nm (C = C) corresponding to benzyl alcohol. Ethyl benzoate molecules adsorbed onto the surface of GNSs and were subsequently reduced by AuNCs catalysis, therefore, the GNS-AuNCs hybrid shows enhanced catalytic efficiency towards ethyl benzoate reduction. The proposed reduction mechanism is supported by the catalysis results and a study on nitroarene reduction catalyzed by a GO-AuNCs hybrid.[53] Importantly, the product benzyl alcohol is a core moiety in several anti-tumor bioactive molecules (Figure 6d).[54] Thus we have demonstrated the high-performance of GNS-AuNCs hybrid as an active catalyst for ethyl benzoate reduction.

3. Conclusions

In summary, an efficient in situ solution-processed aqueous glycine-bisulfate ionic-complex-assisted electrochemical exfoliation method for the synthesis of GNSs was developed. The method has major advantages over existing methods, such as a) environmental friendliness, b) low cost, c) facile operational procedure, d) efficient exfoliation, e) low operational voltages (+1 V for 5 min and +3 V for 5 min), f) one-pot soft processing approach, g) formation of high-quality, few-layer GNSs with a yield of 2.2 g L^{-1}, and h) an observed highly catalytic efficiency when employed GNS-AuNCs hybrid for benzoate reduction. The proposed exfoliation mechanism involves the formation of surface molecule nuclei via the polymerization of intercalated ions and the reduction of ionic species that form large $(SO_2)_n$ gas bubbles, which create large forces inside graphite layers, leading to effective exfoliation. The present method is useful for the development of new graphene-based materials for future technological applications.

4. Experimental Section

Materials: All chemicals were used as received from Sigma-Aldrich. High-purity graphite rods (99.9995%, 6.15 mm in diameter, 152 mm in length) were obtained from Alfa Aesar. HPLC-grade solvents were used in this study. Aqueous solutions were purified using Milli-Q water (>18.2 MΩ) by a Roda purification system (Te Chen Co. Ltd).

Preparation of GNSs: The Gly·HSO_4 ionic complex was prepared using a standard procedure.[35] Typically, glycine (1.30 g, 17.3 mmol) is dissolved in 75 mL of water and sulfuric acid (1.69 g, 17.3 mmol) was slowly added, then reaction proceeds for a period of 1 h at room temperature. Throughout the procedure the solution was kept stirring. The reaction produces a 4:96 weight ratio of Gly·HSO_4/H_2O. To perform the exfoliation experiments, a graphite rod as anode was placed in parallel to a platinum sheet cathode in the above solution with a gap of 3 cm. The applied static potentials were managed using a DC power supply potentiostat (TES-6200, USA). The exfoliation experiments were conducted at ambient conditions. After an appropriate time, a black precipitate was collected through 100-nm porous filters, washed with excess aqueous solution and ethanol, and then re-dispersed into NMP solvent using water-bath sonication for 10 min. The resulting graphene dispersion was directly used for further characterizations. These exfoliation experiments can also be conducted using graphite rod anode with graphite rod or Al or Ni electrode[29] as the cathode. The experimental procedure of reduction catalysis is same as we reported in the elswhere.[52]

Characterizations: The structural investigation and surface morphology analysis of GNS15 was carried out using HR-TEM (JEOL, JSM-2100F) with an acceleration voltage of 200 kV. The XPS analysis was performed using PHI Quantera SXM (ULVAC Inc.) to measure the binding energies of carbon and oxygen. A confocal Raman spectrometer (Renishaw inVia) was used to collect Raman spectra (laser wavelength of 633 nm and laser power of 8 mW cm^{-2}). The Si peak at 520 cm^{-1} was used as a reference for wavenumber calibration. FT-IR spectra in a range of 400 to 4000 cm^{-1} were collected using an FT-IR spectrometer (VERTEX 70, Bruker, Germany). Samples used for TEM measurements were prepared by drop-casting onto lacey-carbon-coated Cu grids followed by an drying step (60 °C for 30 min). The samples for Raman and XPS spectroscopy were prepared by drop-casting onto a glass substrate followed by an drying step (60 °C for 30 min). The KBr disc method was used for the preparation of FT-IR samples. The concentration of the GNS dispersion was analyzed as follows: 100 µL of GNS dispersion in a pre-weighted differential scanning calorimetry (DSC) crucible was evaporated under vacuum (50 °C, 3 days). The final weight of dry GNS was calculated.

Supporting Information

Supporting Information is available from the Wiley Online Library or from the author.

Acknowledgements

The authors are grateful to Prof. Yury Gogotsi, Department of Materials Science and Engineering and A.J. Drexel Nanotechnology Institute, Drexel University for valuable discussion. The authors gratefully acknowledge professors Jiunn-Der Liao, Jyh-Ming Ting, and Mario Hofmann, Dr. Stuart Thomas, Dr. Yung-Fang Liu, Dr. Wan-Hsien Lin, and research student Pei-Ru So for their support. The research project was supported by a grant from National Cheng Kung University, Taiwan.

Received: August 3, 2014
Revised: October 19, 2014
Published online: November 20, 2014

[1] M. I. Katsnelson, K. S. Novoselov, A. K. Geim, *Nat. Phys.* **2006**, *2*, 620.
[2] K. S. Novoselov, Z. Jiang, Y. Zhang, S. V. Morozov, H. L. Stormer, U. Zeitler, J. C. Maan, G. S. Boebinger, P. Kim, A. K. Geim, *Science* **2007**, *315*, 1379.
[3] F. Wang, Y. Zhang, C. Tian, C. Girit, A. Zettl, M. Crommie, Y. R. Shen, *Science* **2008**, *320*, 206.
[4] C. Lee, X. D. Wei, J. W. Kysar, J. Hone, *Science* **2008**, *321*, 385.
[5] R. S. Ruoff, *MRS Bulletin* **2012**, *37*, 1314.
[6] R. Hawaldar, P. Merino, M. R. Correia, I. Bdikin, J. Grácio, J. Méndez, J. A. Martín-Gago, M. K. Singh, *Sci. Rep.* **2012**, *2*, 682.
[7] J.-C. Yoon, J.-S. Lee, S.-I. Kim, K.-H. Kim, J.-H. Jang, *Sci. Rep.* **2013**, *3*, 1788.
[8] F. Bonaccorso, A. Lombardo, T. Hasan, Z. Sun, L. Colombo, A. C. Ferrari, *Mater. Today* **2012**, *15*, 564.
[9] K. S. Novoselov, V. I. Fal'ko, L. Colombo, P. R. Gellert, M. G. Schwab, K. Kim, *Nature* **2012**, *490*, 192.
[10] T. Hasan, F. Torrisi, Z. Sun, D. Popa, V. Nicolosi, G. Privitera, F. Bonaccorso, A. C. Ferrari, *Phys. Status Solidi B* **2010**, *247*, 2953.
[11] V. Chabot, B. Kim, B. Sloper, C. Tzoganakis, A. Yu, *Sci. Rep.* **2013**, *3*, 1378.
[12] S. Park, R. S. Ruoff, *Nat. Nanotechnol.* **2009**, *4*, 217.
[13] C.-H. Zhu, Y. Lu, J. Peng, J. Chen, S.-H. Yu, *Adv. Funct. Mater.* **2012**, *22*, 4017.
[14] J. Senthilnathan, K. Sanjeeva Rao, M. Yoshimura, *J. Mater. Chem. A* **2014**, *2*, 3332.
[15] S. Stankovich, S. Stankovich, D. A. Dikin, G. H. B. Dommett, K. M. Kohlhaas, E. J. Zimney, E. A. Stach, R. D. Pine, S. T. Nguyen, R. S. Ruoff, *Nature* **2006**, *442*, 282.
[16] D. A. Dikin, S. Stankovich, E. J. Zimney, R. D. Piner, G. H. B. Dommett, G. Evmenenko, S. T. Nguyen, R. S. Ruoff, *Nature* **2007**, *448*, 457.
[17] V. C. Tung, L.-M. Chen, M. J. Allen, J. K. Wassei, K. Nelson, R. B. Kaner, Y. Yang, *Nano Lett.* **2009**, *9*, 1949.
[18] H. Hu, Z. Zhao, W. Wan, Y. Gogotsi, J. Qiu, *Adv. Mater.* **2013**, *25*, 2219.
[19] H. Hu, Z. Zhao, Q. Zhou, Y. Gogotsi, J. Qiu, *Carbon* **2012**, *50*, 3267.
[20] O. M. Marago, F. Bonaccorso, R. Saija, G. Privitera, P. G. Gucciardi, M. A. Iatì, G. Calogero, P. H. Jones, F. Borghese, P. Denti, V. Nicolosi, A. C. Ferrari, *ACS Nano* **2010**, *4*, 7515.
[21] X. Wang, L. Jiao, K. Sheng, C. Li, L. Dai, G. Shi, *Sci. Rep.* **2013**, *3*, 1996.
[22] J. Senthilnathan, Y.-F. Liu, K. Sanjeeva Rao, M. Yoshimura, *Sci. Rep.* **2014**, *4*, 4395.
[23] N. Liu, F. Luo, H. Wu, Y. Liu, C. Zhang, J. Chen, *Adv. Funct. Mater.* **2008**, *18*, 1518.
[24] J. Lu, J.-X. Yang, J. Wang, A. Lim, S. Wang, K. P. Loh, *ACS Nano* **2009**, *3*, 2367.
[25] M. Mao, M. Wang, J. Hu, G. Lei, S. Chen, H. Liu, *Chem. Commun.* **2013**, *49*, 5301.
[26] Z. Y. Xia, S. Pezzini, E. Treossi, G. Giambastiani, F. Corticelli, V. Morandi, A. Zanelli, V. Bellani, V. Palermo, *Adv. Funct. Mater.* **2013**, *23*, 4684.
[27] G. M. Morales, P. Schifani, G. Ellis, C. Ballesteros, G. Martínez, C. Barbero, H. J. Salavagione, *Carbon* **2011**, *49*, 2809.
[28] J. Liu, C. K. Poh, D. Zhan, L. Lai, S. H. Lim, L. Wang, X. Liu, N. G. Sahoo, C. Li, Z. Shen, J. Lin, *Nano Energy* **2013**, *2*, 377.
[29] J. Wang, K. K. Manga, Q. Bao, K. P. Loh, *J. Am. Chem. Soc.* **2011**, *133*, 8888.
[30] Y. L. Zhong, T. M. Swager, *J. Am. Chem. Soc.* **2012**, *134*, 17896.
[31] K. Sanjeeva Rao, J. Senthilnathan, Y.-F. Liu, M. Yoshimura, *Sci. Rep.* **2014**, *4*, 4237.
[32] C.-Y. Su, A.-Y. Lu, Y. Xu, F.-R. Chen, A. Khlobystov, L.-J. Li, *ACS Nano* **2011**, *5*, 2332.
[33] M. Alanyalıoglu, J. J. Segura, J. Oró-Solè, N. Casañ-Pastor, *Carbon* **2012**, *50*, 142.
[34] H. Huang, Y. Xia, X. Tao, J. Du, J. Fang, Y. Gan, W. Zhang, *J. Mater. Chem.* **2012**, *22*, 10452.
[35] L.-L. Dong, L. He, G.-H. Tao, C. Hu, *RSC Adv.* **2013**, *3*, 4806.
[36] G. H. Tao, L. He, N. Sun, Y. Kou, *Chem. Commun.* **2005**, *28*, 3562.
[37] G.-H. Tao, L. He, W.-S. Liu, L. Xu, W. Xiong, T. Wang, Y. Kou, *Green Chem.* **2006**, *8*, 639.
[38] M. Yoshimura, *J. Mater. Sci.* **2006**, *41*, 1299.
[39] S. Bose, T. Kuila, A. K. Mishra, N. H. Kim, J. H. Lee, *J. Mater. Chem.* **2012**, *22*, 9696.
[40] C. Ferrari, J. Robertson, *Phys. Rev. B* **2000**, *61*, 14095.
[41] L. G. Cancado, A. Jorio, E. H. M. Ferreira, F. Stavale, C. A. Achete, R. B. Capaz, M. V. O. Moutinho, A. Lombardo, T. S. Kulmala, A. C. Ferrari, *Nano Lett.* **2011**, *11*, 3190.
[42] A. C. Ferrari, J. C. Meyer, V. Scardaci, C. Casiraghi, M. Lazzeri, F. Mauri, S. Piscanec, D. Jiang, K. S. Novoselov, S. Roth, A. K. Geim, *Phys. Rev. Lett.* **2006**, *97*, 187401.
[43] Y. Li, M. V. Zijll, S. Chiang, N. Pan, *J. Power Sources* **2011**, *196*, 6003.
[44] S. Park, J. An, R. D. Piner, I. Jung, D. Yang, A. Velamakanni, S. T. Nguyen, R. S. Ruoff, *Chem. Mater.* **2008**, *20*, 6592.
[45] S. Yumitori, *J. Mater. Sci.* **2000**, *35*, 139.
[46] G.-X. Zhu, X.-W. Wei, S. Jiang, *J. Mater. Chem.* **2007**, *17*, 2301.
[47] K. S. Novoselov, A. K. Geim, S. V. Morozov, D. Jiang, Y. Zhang, S. V. Dubonos, I. V. Grigorieva, A. A. Firsov, *Science* **2004**, *306*, 666.

[48] J. A. Seel, J. R. Dahn, *J. Electrochem. Soc.* **2000**, *147*, 892.
[49] W. Katinaonkul, M. M. Lerner, *J. Fluorine Chem.* **2007**, *128*, 332.
[50] K. Parvez, Z.-S. Wu, R. Li, X. Liu, R. Graf, X. Feng, K. Müllen, *J. Am. Chem. Soc.* **2014**, *136*, 6083.
[51] L. Shi, Y. Liu, Q. Liu, B. Wei, G. Zhang, *Green Chem.* **2012**, *14*, 1372.
[52] K. Sanjeeva Rao, J. Senthilnathan, J.-M. Ting, M. Yoshimura, *Nanoscale* **2014**, *6*, 12758.
[53] Y. Choi, H. S. Bae, E. Seo, S. Jang, K. H. Park, B.-S. Kim, *J. Mater. Chem.* **2011**, *21*, 15431.
[54] J. S. Yadav, B. M. Rao, K. Sanjeeva Rao, B. V. S. Reddy, *Synlett* **2008**, *7*, 1039.